materials

MDPI

Article

Investigating the Size-Dependent Binding of Pristine nC_{60} to Bovine Serum Albumin by Multi-Spectroscopic Techniques

Shufang Liu *, Shu'e Wang and Zhanzuo Liu

School of Public Health, Cheeloo College of Medicine, Shandong University, Wenhuaxi Road 44, Jinan 250012, China; wse@sdu.edu.cn (S.W.); liuzhanzuo2021@163.com (Z.L.)
* Correspondence: liushufang@sdu.edu.cn

Abstract: The morphology of nanomaterials may affect their interaction with biomacromolecules such as proteins. Previous work has studied the size-dependent binding of pristine nC_{60} to bovine/human serum albumin using the fluorometric method and found that the fluorescence inner filter effect might affect this interaction. However, if it is necessary to accurately calculate and obtain binding information, the fluorescence inner filter effect should not be ignored. This work aimed to further investigate the effect of the fluorescence inner filter on the interaction between pristine nC_{60} with different particle sizes (140–160, 120–140, 90–110, 50–70, and 30–50 nm) and bovine serum albumin for a more accurate comprehension of the binding of pristine nC_{60} to bovine serum albumin. The nC_{60} nanoparticles with different size distributions used in the experiments were obtained by the solvent displacement and centrifugation method. UV-Vis spectroscopy and fluorescence spectroscopy were used to study the binding of nC_{60} with different size distributions to bovine serum albumin (BSA) before and after eliminating the fluorescence inner filter effect. The results showed that the fluorescence inner filter effect had an influence on the interaction between nC_{60} and proteins to some extent, and still did not change the rule of the size-dependent binding of nC_{60} nanoparticles to BSA. Further studies on the binding parameters (binding constants and the number of binding sites) between them were performed, and the effect of the binding on BSA structures and conformation were also speculated.

Keywords: nC_{60}; fullerene; bovine serum albumin; inner filter effect; fluorescence

Citation: Liu, S.; Wang, S.; Liu, Z. Investigating the Size-Dependent Binding of Pristine nC_{60} to Bovine Serum Albumin by Multi-Spectroscopic Techniques. *Materials* **2021**, *14*, 298. https://doi.org/10.3390/ma14020298

Received: 7 December 2020
Accepted: 5 January 2021
Published: 8 January 2021

1. Introduction

As a kind of classic carbon nanomaterial, due to their unique structural characteristics and physical and chemical properties, nC_{60} nanomaterials and their derivatives have great application potential in many fields, such as chemistry, life sciences, materials sciences, and biomedicine. [1–3]. Therefore, research on their safety and biological effects has also attracted great attention, in which the interaction between nC_{60} (and its derivatives, most of which are water-soluble, such as fullerol, carboxylic acid, and amine) and proteins is an important part of their biological effects, and detailed comprehension of their interactions with proteins is fundamentally important for their future biomedical applications.

Previous studies have shown that nC_{60} and its derivatives can bind to a variety of proteins (peptides) and change their conformation and structure, and the morphological characteristics of nC_{60} and its derivatives have a certain effect on these bindings [4–12]. Since unmodified nC_{60} is not soluble in water, most of the studies were on water-soluble nC_{60} derivatives. However, due to the limitation of experimental methods, the types and quantity of modification groups of nC_{60} derivatives obtained by different research groups are different, which leads to the lack of comparability of data among different research groups. Even for the study of the interaction between pristine nC_{60} and proteins, due to the different preparation methods of nC_{60} nanoparticles, the morphology characteristics (morphology, size, particle size distribution, surface area, etc.) of nC_{60} aqueous dispersion

obtained by different research groups are also different, so the research results of different research groups are not completely consistent.

In our previous work, in order to eliminate other factors of the interaction, we obtained nC_{60} with different particle sizes by the centrifugation method, and confirmed the size-dependent binding of pristine nC_{60} to human serum albumin (HSA)/bovine serum albumin (BSA) by fluorescence quenching spectroscopy [13]. However, the binding details and mechanism need to be further discussed.

To quantify the binding of small molecules/nanoparticles to proteins, several homogeneous methods have been developed, such as isothermal titration calorimetry (ITC) [14], fluorescence quenching or enhancement [15], fluorescence polarization (FP) [16], and Förster resonance energy transfer (FRET) [17], among which the fluorescence method has been widely used because of its high sensitivity and selectivity, simplicity, and rapidity. As an important and effective method of fluorescence analysis, fluorescence quenching plays a prominent role in studying the interaction between biological macromolecules and coexisting substances. However, when the fluorescent molecules interact with coexisting substances such as small molecules/nanoparticles, the fluorescence inner filter effect is often neglected, and thus a rough or even incorrect conclusion may be drawn.

If there are small molecules or other substances in the solution that can absorb the excitation light (primary inner filter effect) or the emission light of fluorescence substances (secondary inner filter effect), the fluorescence is weakened, which is called the inner filter effect (IFE) [14,18]. The IFE was previously considered an error in fluorescence measurement, but due to its simple operation and high sensitivity, as well as the lack of a need to modify the donor or connect the donor with the receptor, it has been widely used in the detection of enzyme activity, pesticides, metabolites, small molecule chemicals, etc. [19–21].

In our previous work, we found that particle size has an obvious effect on the binding of nC_{60} to HSA and BSA. nC_{60} nanoparticles with smaller size distribution have stronger binding to HSA/BSA proteins. At a lower concentration, considering the low absorption intensity of nC_{60} in the UV-Vis region, the existence of the inner filter effect does not change the size-dependent binding of nC_{60} to proteins. However, if we need to further clarify the law of the nanoparticle size on the interaction between nC_{60} and proteins, and then judge the mechanism of the interaction, the inner filter effect should be involved and deducted in the calculation.

Based on the research background of the interaction between nC_{60} (and its derivatives) and proteins, to further understand the influence of particle size on the interaction between nC_{60} and proteins, and to obtain the mechanism of the interaction, we further studied the inner filter effect on the interaction between nC_{60} and several proteins, and discussed the possible mechanism of said interaction. On the basis of the obtained binding information, the effect of the binding on BSA structures and conformation were also speculated.

2. Experimental Methods

2.1. Materials

C_{60} powder (purity 99.9%) was purchased from Henan Puyang Yongxin Fullerene Technology Co. Ltd. (Puyang, China). BSA, HSA (free fatty acid fraction V), and phosphate buffer saline (PBS) premixed powder (pH = 7.2–7.4) were obtained from Sigma-Aldrich ((St Louis, MO, USA). During the experiments, the nC_{60} dispersions were kept away from light. Distilled ultra-pure water (18.3 MΩ) was obtained from the Milli-Q plus system (Millipore, Bedford, MA, USA) and used in all experiments. All of the experiments were performed at room temperature.

2.2. Instruments

A UV-2450 spectrophotometer (Shimadzu, Tokyo, Japan), HT-7700 transmission electron microscopy (TEM) (Hitachi, Tokyo, Japan), and a FL-4500 spectrofluorometer equipped with an Xe lamp as a excitation light source (Hitachi, Japan) were used.

2.3. Preparation and Characterization of nC_{60} Dispersions

Stock aqueous dispersion of nC_{60} nanoparticles and nC_{60} dispersions with different particle size distributions were prepared by the centrifugal method according to our previously published work [13]. According to the different centrifugal velocities, 5 nC_{60} dispersions with different particle sizes were finally obtained and named S_{4b}, S_0, S_4, S_8, and S_{12}, and the average size distributions of 5 dispersions was in the order of $S_{4b} > S_0 > S_4 > S_8 > S_{12}$ (S_{4b}: 140–160 nm, S_0: 120–140 nm, S_4: 90–110 nm, S_8: 50–70 nm, and S_{12}: 30–50 nm) [13].

2.4. Fluorescence Spectra Measurements of Proteins

A protein stock solution of 0.5 mL (1.0×10^{-4} mol/L) and an nC_{60} dispersion of different volumes was added to 5 colorimetric tubes with a volume of 10 mL in order to obtain a series of concentrations of nC_{60}–protein mixture dispersions, then the volume was fixed to 5 mL with PBS buffer, and the 5 mixtures were thoroughly mixed.

The fluorescence spectra measurements of the above 5 mixtures were performed on an FL-4500 spectrofluorometer equipped with a 1.0 cm quartz cell (laser source: Xe lamp; λex = 280 nm; excitation and emission slit width: 5 nm; scan speed: 1200 nm/min; photomultiplier tube (PMT) voltage: 700 V), and the intensity values at the maximum fluorescence emission wavelength of BSA were recorded. All of the measurements were done at room temperature.

2.5. Determination of Absorbance of nC_{60}–Protein Systems

The determination of the UV-Vis absorbance of the 5 mixtures at 280 nm and 330 nm in the experiments were performed on a UV-2450 spectrophotometer equipped with a 1.0 cm quartz cell (scan speed: medium). All of the measurements were done at room temperature.

2.6. Mathematical Correction

For protein–nC_{60} systems, the following mathematical correction formula was used to correct the fluorescence data obtained [22]:

$$F_{corr} = F_{obs} \times e^{(A_{ex}+A_{em})/2} \quad (1)$$

In the formula, F_{obs} is the maximum fluorescence intensity without internal filtering effect correction; F_{corr} is the maximum fluorescence intensity after internal filtering effect correction; A_{ex} is the absorption value of the mixed solution at the excitation wavelength (λex = 280 nm); A_{em} is the absorption value of the mixed solution at the emission wavelength (λem = 340 nm).

2.7. Determination of the Surface Hydrophobicity Index (SHI) of BSA

A buffer of 5 mL of 0.04 mol/L PBS and 0.10, 0.25, 0.50, 1.00, or 2.00 mL of BSA were added to 10 mL colorimetric tubes. An appropriate amount of nC_{60} with different particle sizes was added to each tube, and the volume was fixed with distilled water to 5 mL; the final concentration of nC_{60} with different particle sizes in each tube was fixed at 9.68×10^{-6} mol/L (relatively high concentration). The mixture was mixed well and reacted in the dark for 5 min at room temperature. The excitation wavelength was set at 380 nm, and the fluorescence emission spectrum (420–550 nm) was determined by scanning the above solution. In the presence of an excessive fluorescent probe (8-anilino-1-naphthalene sulfonate (ANS)), the slope of the straight line obtained by plotting the fluorescence intensity at 470 nm against the BSA concentration was the surface hydrophobicity index (SHI) of BSA.

3. Results and Discussion

3.1. The Existence of Fluorescence Inner Filter Effect in nC_{60}–Protein (HSA/BSA) Systems

Fluorescence spectroscopy is often used to study the interaction between proteins and other substances [15,23]. In previous studies, we used the fluorescence method to study the interaction between nC_{60} and several proteins. It was found that nC_{60} can quench the fluorescence of proteins (BSA and HSA) with a dose–response relationship, and the smaller the particle size of nC_{60}, the stronger its ability to quench protein fluorescence [13]. However, by scanning the UV absorption spectrum of nC_{60} and the fluorescence emission spectrum of protein (BSA and HSA, λex = 280 nm), there was an overlap between them (Figure 1). This means that nC_{60} might have absorbed the excitation light and the emission light of the proteins, the so-called fluorescence internal filtering phenomenon, and thus, the fluorescence intensity of the proteins decreased. Due to the low concentration ranges and the weak absorbance of the nC_{60} nanoparticles in the experiment, the effect of the fluorescence inner filter on the size-dependent binding law of nC_{60} to the proteins was small and can be neglected [13]. However, to calculate the binding constant and the number of binding sites of the interaction between nC_{60} and the proteins, and to comprehend the mechanism of the interaction, the influence of the inner filter had to be considered and deducted.

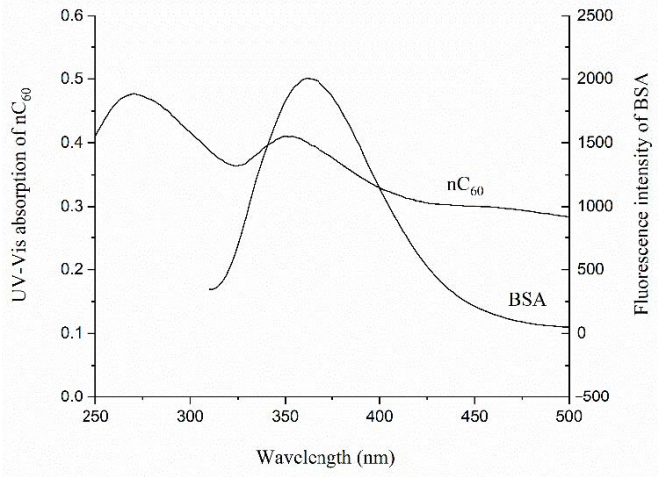

Figure 1. The overlap between the UV absorption spectrum of nC_{60} and the fluorescence emission spectrum of proteins (bovine serum albumin (BSA)).

3.2. Calculation of the Fluorescence Inner Filter Effect in the System

In order to comprehend the fluorescence inner filter effect on the interaction between nC_{60} with different particle sizes and BSA, we used Formula (1) for fluorescence correction, and obtained the fluorescence quenching plots of BSA by nC_{60} before correction (a) [13] and after correction (b) of the fluorescence inner filter effect (Figure 2).

Figure 2 shows that the SternVolmer plots for the fluorescence of BSA by nC_{60} was a curve bending to the *Y*-axis before the inner filter effect was corrected. After the correction of the inner filter effect, at the same concentration of nC_{60} nanoparticles, the degree of fluorescence quenching of the proteins decreased to a certain extent, and the Stern–Volmer plots still approached curves bending to the *Y*-axis, while the size-dependent quenching effect of nC_{60} on BSA remained unchanged.

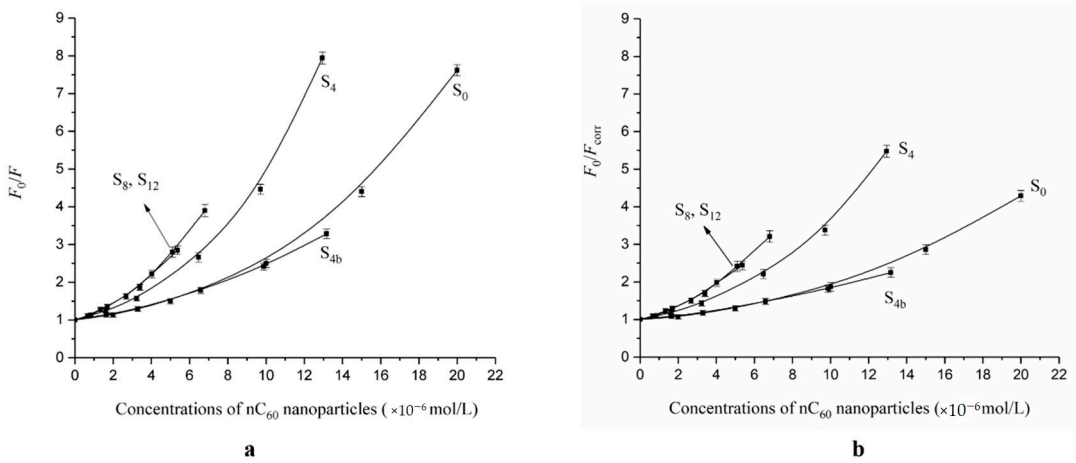

Figure 2. The fluorescence quenching plots of BSA by nC_{60} with (**a**) and without (**b**) correction of the fluorescence inner filter effect.

3.3. The Binding Constants and Binding Sites of nC_{60} Nanoparticles to BSA

Due to the different quenching mechanisms, the fluorescence quenching mainly included dynamic quenching and static quenching. Dynamic quenching refers to the collision between the quenching agent and the excited-state fluorescence molecules during the fluorescence lifetime, which caused the fluorescence molecule to return from the excited state to the ground state in the way of non-radiative transition without emitting fluorescence, resulting in the fluorescence quenching effect of fluorescence molecule. This process can be described by the Stern–Volmer linear equation [24]:

$$F_0/F = 1 + k_q\tau_0 c = 1 + K_{sv}c$$

In the equation, F_0 and F represent the fluorescence intensity at the maximum emission wavelength of BSA fluorescence spectra in the absence and presence of a quenching agent, respectively; τ_0 is the average fluorescence lifetime of fluorescence molecules (such as biomacromolecules) in the absence of a quenching agent, generally 10^{-8} *s*; K_{SV} is the dynamic quenching constant (L/mol); c is the concentration of the added quenching agent (mol/L); k_q is the dynamic quenching rate constant (L/(mol·s)), and the maximum dynamic quenching rate constant of various fluorescence quenching agents for biomacromolecule is approximately 2.0×10^{10} (L/(mol·s)) [12].

Assuming the fluorescence quenching mechanism of nC_{60} to BSA belongs to dynamic quenching, the Stern–Volmer plots were drawn after correction of the inner filter effect (Figure 2). The corrected Stern–Volmer plots are rising curves bending to the vertical axis, which indicate that either both dynamic quenching and static quenching occurred between nC_{60} and BSA at the same time, or single static quenching occurred [24].

For the fluorescence quenching caused by the combination of dynamic and static quenching, the retained fluorescence fraction (F/F_0) is the product of the fraction of the uncomplexed fluorescence molecules and the fraction of the fluorescence molecules not quenched by the collision encounter:

$$\frac{F}{F_0} = f\frac{\gamma}{\gamma + k_q[Q]} \quad (2)$$

In the equation, $\gamma = \frac{1}{\tau_0}$, where $[Q]$ is the concentration of the quenching agent. Take the reciprocal of the above formula and rearrange it to get:

$$\frac{F_0}{F} = \frac{1}{f}(1 + k_q\tau_0[Q]) \quad (3)$$

$$\frac{F_0}{F} = \frac{1}{f}(1 + K_{SV}[Q]) \tag{4}$$

If static quenching occurs between the quenching agent (Q) and the fluorescent molecules (M), it is assumed that a ground-state complex is formed between the quenching agent (Q) and the fluorescent molecules (M) as MQ_n, namely:

$$nQ + M \leftrightarrow MQ_n$$

The binding constant (K) between the quenching agent and the fluorescent molecules can be expressed as:

$$K = \frac{[MQ_n]}{[M][Q]^n} \tag{5}$$

According to the relationship between fluorescence intensity and quenching agent concentration, it can be deduced as follows:

$$[M]_0 = [M] + [MQ_n] \tag{6}$$

$$\frac{F_0 - F}{F} = \frac{[M]_0 - [M]}{[M]} = \frac{[MQ_n]}{[M]} = K[Q]^n \tag{7}$$

Rearrange Equation (6) to get Equation (7):

$$\frac{F_0}{F} = 1 + K[Q]^n \tag{8}$$

If the quenching behavior of the quenching agent to the fluorescence molecules belongs to static quenching, the fraction of the fluorescence molecules that has not been complexed (f) can be expressed as follows:

$$f = \frac{F}{F_0} = \frac{1}{1 + K[Q]^n} \tag{9}$$

In Equation (6), $[M]_0$ is the total concentration of fluorescent molecules, [M] is the concentration of uncomplexed fluorescent molecules, and [MQ_n] is the concentration of ground-state complexes generated by the quenching agent and fluorescent molecules.

From Equations (3) and (8), Equation (9) can be deduced:

$$\frac{F_0}{F} = \frac{1}{f}(1 + K_{SV}[Q]) = (1 + K[Q]^n)(1 + K_{SV}[Q]) \tag{10}$$

Namely:

$$(\frac{F_0}{F} - 1) = K_{SV}[Q] + K[Q]^n + K_{SV}K[Q]^{n+1} \tag{11}$$

A curve can be obtained by drawing $(\frac{F_0}{F} - 1)$ to $[Q]$, and the values of K_{SV}, K, and n can be obtained by simulating the curve with the nonlinear fitting function of Origin software.

Using the above method (the obtained fitting curves shown in Figure 2), the parameters (K_{SV}, K, and n) of the interaction between nC_{60} with different particle sizes and BSA could be obtained (Table 1).

From Table 1, the K_{sv} was in a range of 2.35×10^4–12.1×10^4 L/mol, and the K_q was in a range of 1.21×10^{12}–7.25×10^{12} L/(mol·s), which was much larger than the maximum diffusion collision quenching constant (2.0×10^{10} L/(mol·s)) of various quenchers on biomacromolecules, indicating that the fluorescence quenching mechanism of nC_{60} for BSA was mainly static quenching. The number of binding sites (n) ranged from 1.39 to 2.41, indicating that 1–2 C_{60} molecules might be bound to one BSA molecule.

Table 1. The parameters (K_{SV}, K, n, and K_q) of the interaction between nC_{60} and BSA.

nC_{60}	Binding Parameters of nC_{60} to BSA				R^2 (COD)
	K_{SV} ($\times 10^4$ L/mol)	K ($\times 10^8$ L/mol)	n	K_q ($\times 10^{12}$ L/(mol·s))	
S_{12}	7.25	0.20	1.41	7.25	0.998
S_8	5.13	1.15	1.53	5.13	0.998
S_4	12.1	7015.84	2.41	1.21	0.999
S_0	2.88	15.37	1.90	2.88	0.999
S_{4b}	2.35	0.05	1.39	2.35	0.999

Actually, the sizes of five nC_{60} nanoparticle dispersions were 40–160, 120–140, 90–110, 50–70, and 30–50 nm, respectively, which were much larger than the protein molecules. Therefore, it was difficult to incorporate nC_{60} into the binding pocket of BSA. According to the previously reported atomistic computer simulations of some albumin subdomains on a hydrophobic graphite surface [25], it was proposed that BSA might be absorbed on the surface of an nC_{60} aggregate, which caused the fluorescence quenching. According to the quenching synchronous fluorescence spectrometry, the binding site of nC_{60} to BSA was located near the tryptophan residues, indicating the conformation change of BSA.

From the BSA fluorescence quenching plots by nC_{60}, with or without correcting the fluorescence inner filter effect, the apparent size-dependent binding of nC_{60} to BSA could be observed (Figure 2). At the same concentration of nC_{60}, the smaller the particle size, the stronger the fluorescence quenching ability of BSA. However, interestingly, after deducting the fluorescence internal filtering effect, by calculating the binding parameters of BSA and nC_{60} with different particle sizes, it can be seen that this was not the case. It was actually more complicated. Table 1 shows that S_4 had the strongest binding ability (K) to BSA and the largest number of binding sites (n), followed by S_0, and that S_{4b} was the weakest. According to the size distribution of the nC_{60} nanoparticles characterized by TEM in our previous work [13], it can be speculated that compared with other particle sizes, nC_{60} nanoparticles of approximately 100 nm bind more easily to BSA because they are more sensitive to binding.

3.4. Effect of nC_{60} with Different Size Distributions on the Surface Hydrophobicity of BSA and Speculation of Their Binding Sites

In order to further understand the effect of nC_{60} nanoparticles on BSA conformation and to speculate their binding sites with BSA, the effect of nC_{60} on the surface hydrophobicity of BSA was studied using the fluorescence probe method. 8-anilino-1-naphthalene sulfonate (ANS) is a common fluorescent probe, which can be non-covalently bound to the non-polar region of proteins. Its fluorescence spectrum is blue-shifted with an increase in the non-polar environment, and its fluorescence intensity also increases and shows a linear relationship with the concentration of proteins. Therefore, by determining the polarity change of the binding sites of proteins, a change of hydrophobicity and protein structure can be speculated [26,27]. In this experiment, the concentration of nC_{60} with different particle sizes was fixed at 9.68×10^{-6} mol/L (relatively high concentration), and their effects on the BSA surface hydrophobicity using the ANS fluorescence probe method were observed (Figure 3).

Figure 3 shows how, after adding the same concentration of nC_{60} with different particle sizes to a BSA solution, the surface hydrophobicity of BSA decreased slightly, but the effect of nC_{60} with different particle sizes on the hydrophobicity of BSA was not significant, and there were no obvious effect of nC_{60} particle size.

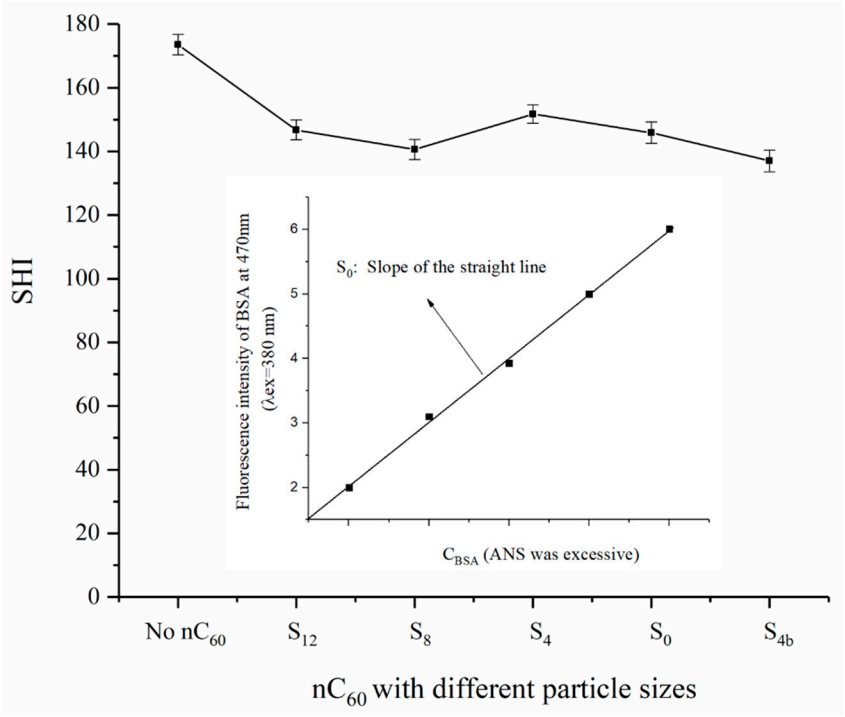

Figure 3. The BSA surface hydrophobicity determined using the ANS fluorescence probe method in the absence and presence of nC_{60} nanoparticles.

Previous work by synchronous fluorescence spectrometry has proved that the binding site of nC_{60} to BSA is located in the vicinity of tryptophan residues [13,28], and that the effect of nC_{60} with different particle sizes (at lower nC_{60} concentrations) on the microenvironment around tryptophan residue is also different [13]. Similarly, if the concentration of nC_{60} with different particle sizes was fixed at 9.68×10^{-6} mol/L, it could be seen that the influence of nC_{60} with different particle sizes on the fluorescence emission wavelength of BSA was different. The smaller the particle size of nC_{60}, the more likely was a red shift of the maximum fluorescence emission wavelength of BSA, while the larger the particle size of nC_{60}, the more likely was a blue shift of the maximum fluorescence emission wavelength of BSA.

Therefore, according to the experimental results of this work and our previous work, it can be speculated that the binding site of nC_{60} and BSA was closer to the position of tryptophan residues, which caused a polarity change of microenvironment around amino acid residues, and this change showed a relatively obvious size effect of nC_{60}. However, the polarity change of the microenvironment around amino acid residues had little effect on the structure of BSA, and had no obvious size effect on the nC_{60} nanoparticles.

4. Conclusions

In this work, the size-dependent binding of nC_{60} to BSA was further calculated using the spectroscopic method. It was found that although nC_{60} with different particle sizes could quench the fluorescence of BSA with a certain particle size effect, the nC_{60} with a particle size of approximately 100 nm was easier to bind to BSA with a relatively stronger binding constant and a larger number of binding sites, which may be due to the fact that nC_{60} of this size was more suitable for its binding in the cavity around the tryptophan residues of BSA. This conclusion needs further verification, such as molecular docking, and other experimental technologies such as circular dichroism, infrared spectroscopy, Raman spectroscopy, nuclear magnetic resonance spectroscopy, microcalorimetry, laser light scattering, fluorescence polarization technology, and mass spectrometry. In addition, although nC_{60} had a certain effect on the microenvironment around tryptophan residues, it had little effect on the structure of the whole protein molecule and had no obvious particle

size effect of nC_{60}. Due to the characteristics of nanomaterials, many related research works have used the methods of interaction between small molecules and biomacromolecules, so there are some limitations. New research tools need to be developed. In conclusion, this work suggests that the particle size of nanomaterials, including nC_{60}, has an important influence on their binding to biomacromolecules such as proteins, which provides reference for the design and future application of nanomaterials in biomedicine, such as drug carriers.

Author Contributions: S.W. and Z.L. performed the experiments. S.L. conceived and designed the experiments and wrote the manuscript. All authors have read and agreed to the published version of the manuscript.

Funding: This work was supported by a grant from the Youth Program of National Natural Science Foundation of China (no. 81803284) and the Shandong Provincial Natural Science Foundation, China (no. ZR2017MH128).

Institutional Review Board Statement: Not applicable.

Informed Consent Statement: Not applicable.

Data Availability Statement: All data generated or analyzed during this study were included in this article. The original datasets used or analyzed during the current study are available from the corresponding author on reasonable request.

Acknowledgments: The authors greatly acknowledge the Shandong Food Safety Monitoring and Evaluation Engineering Technology Research Center for its support in the use of instruments.

Conflicts of Interest: The authors declare no conflict of interest.

References

1. Kroto, H.W.; Allaf, A.; Balm, S. C60: Buckminsterfullerene. *Chem. Rev.* **1991**, *91*, 1213–1235. [CrossRef]
2. Bakry, R.; Vallant, R.M.; Najam-ul-Haq, M.; Rainer, M.; Szabo, Z.; Huck, C.W.; Bonn, G.K. Medicinal applications of fullerenes. *Int. J. Nanomed.* **2007**, *2*, 639–649.
3. Zakharian, T.Y.; Seryshev, A.; Sitharaman, B.; Gilbert, B.E.; Knight, V.; Wilson, L.J. A fullerene-paclitaxel chemotherapeutic: Synthesis, characterization, and study of biological activity in tissue culture. *J. Am. Chem. Soc.* **2005**, *127*, 12508–12509. [CrossRef] [PubMed]
4. Pochkaeva, E.I.; Meshcheriakov, A.A.; Ageev, S.V.; Podolsky, N.E.; Petrov, A.V.; Charykov, N.A.; Vasina, L.V.; Nikolaeva, O.Y.; Gaponenko, I.N.; Sharoyko, V.V. Polythermal density and viscosity, nanoparticle size distribution, binding with human serum albumin and radical scavenging activity of the C-60-L-arginine (C-60(C6H13N4O2)(8)H-8) aqueous solutions. *J. Mol. Liq.* **2020**, *297*, 111915. [CrossRef]
5. Liu, Z.W.; Zou, Y.; Zhang, Q.W.; Chen, P.J.; Liu, Y.; Qian, Z.Y. Distinct binding dynamics, sites and interactions of fullerene and fullerenols with amyloid-peptides revealed by molecular dynamics simulations. *Int. J. Mol. Sci.* **2019**, *20*, 2048. [CrossRef] [PubMed]
6. Aghaei, M.; Ramezanitaghartapeh, M.; Javan, M.; Hoseininezhad-Namin, M.S.; Mirzaei, H.; Rad, A.S.; Soltani, A.; Sedighi, S.; Lup, A.N.K.; Khori, V.; et al. Investigations of adsorption behavior and anti-inflammatory activity of glycine functionalized Al12N12 and Al12ON11 fullerene-like cages. *Spectrochim. Acta A* **2021**, *246*, 119023. [CrossRef]
7. Bai, C.Q.; Lin, D.D.; Mo, Y.X.; Lei, J.T.; Sun, Y.X.; Xie, L.G.; Yang, X.J.; Wei, G.H. Influence of fullerenol on hIAPP aggregation: Amyloid inhibition and mechanistic aspects. *Phys. Chem. Chem. Phys.* **2019**, *21*, 4022–4031. [CrossRef] [PubMed]
8. Osipov, E.M.; Hendrickson, O.D.; Tikhonova, T.V.; Zherdev, A.V.; Solopova, O.N.; Sveshnikov, P.G.; Dzantiev, B.B.; Popov, V.O. Structure of the Anti-C-60 Fullerene Antibody Fab Fragment: Structural Determinants of Fullerene Binding. *Acta Nat.* **2019**, *11*, 58–65. [CrossRef]
9. Di Giosia, M.; Valle, F.; Cantelli, A.; Bottoni, A.; Zerbetto, F.; Calvaresi, M. C-60 bioconjugation with proteins: Towards a palette of carriers for all pH ranges. *Materials* **2018**, *11*, 691. [CrossRef]
10. Junaid, M.; Almuqri, E.A.; Liu, J.J.; Zhang, H.J. Analyses of the binding between water soluble c60 derivatives and potential drug targets through a molecular docking approach. *PLoS ONE* **2016**, *11*, e0147761. [CrossRef]
11. Yang, L.Y.; Hua, S.Y.; Zhou, Z.Q.; Wang, G.C.; Jiang, F.L.; Liu, Y. Characterization of fullerenol-protein interactions and an extended investigation on cytotoxicity. *Colloid Surf. B* **2017**, *157*, 261–267. [CrossRef] [PubMed]
12. Gieldon, A.; Witt, M.M.; Gajewicz, A.; Puzyn, T. Rapid insight into C60 influence on biological functions of proteins. *Struct. Chem.* **2017**, *28*, 1775–1788. [CrossRef]
13. Fu, X.F.; Fang, Y.L.; Zhao, H.L.; Liu, S.F. Size-dependent binding of pristine fullerene (nC60) nanoparticles to bovine/human serum albumin. *J. Mol. Struct.* **2018**, *1166*, 442–447. [CrossRef]

14. Jelesarov, I.; Bosshard, H.R. Isothermal titration calorimetry and differential scanning calorimetry as complementary tools to investigate the energetics of biomolecular recognition. *J. Mol. Recognit.* **1999**, *12*, 3–18. [CrossRef]
15. Pollard, T.D. A guide to simple and informative binding assays. *Mol. Biol. Cell* **2010**, *21*, 4061–4067. [CrossRef]
16. Jameson, D.M.; Ross, J.A. Fluorescence polarization/anisotropy in diagnostics and imaging. *Chem. Rev.* **2010**, *110*, 2685–2708. [CrossRef]
17. Wu, P.G.; Brand, L. Resonance energy transfer: Methods and applications. *Anal. Biochem.* **1994**, *218*, 1–13. [CrossRef]
18. Kimball, J.; Chavez, J.; Ceresa, L.; Kitchner, E.; Nurekeyev, Z.; Doan, H.; Szabelski, M.; Borejdo, J.; Gryczynski, I.; Gryczynski, Z. On the origin and correction for inner filter effects in fluorescence Part I: Primary inner filter effect the proper approach for sample absorbance correction. *Methods Appl. Fluores* **2020**, *8*, 033002. [CrossRef]
19. Gabor, G.; Walt, D.R. Sensitivity enhancement of fluorescent pH indicators by inner filter effects. *Anal. Chem.* **1991**, *63*, 793–796. [CrossRef]
20. Panigrahi, S.K.; Mishra, A.K. Inner filter effect in fluorescence spectroscopy: As a problem and as a solution. *J. Photochem. Photobiol. C* **2019**, *41*, 100318. [CrossRef]
21. Chen, S.; Yu, Y.L.; Wang, J.H. Inner filter effect-based fluorescent sensing systems: A review. *Anal. Chim. Acta* **2018**, *999*, 13–26. [CrossRef] [PubMed]
22. Steiner, R.F.; Weinryb, I. *Excited States of Protein and Nucleic Acid*; Plenum Press: New York, NY, USA, 1971; p. 40.
23. Tabish, T.A.; Zhang, S.; Winyard, P.G. Developing the next generation of graphene-based platforms for cancer therapeutics: The potental role of reactive oxygen species. *Redox Biol.* **2018**, *15*, 34–40. [CrossRef] [PubMed]
24. Joseph, R.L. *Principles of Fluorescence Spectroscopy*, 3rd ed.; Springer: New York, NY, USA, 2006; pp. 278–281.
25. Raffaini, G.; Ganazzoli, F. Simulation study of the interaction of some albumin subdomains with a flat graphite surface. *Langmuir* **2003**, *19*, 3403–3412. [CrossRef]
26. Haskard, C.A.; Li-Chan, E.C.Y. Hydrophobicity of bovine serum albumin and ovalbumin determined using uncharged (PRODAN) and anionic (ANS-). *J. Agric. Food Chem.* **1998**, *46*, 2671–2677. [CrossRef]
27. Alizadeh-Pasdar, N.; Li-Chan, E.C.Y. Comparison of protein surface hydrophobicity measured at various pH values using three different fluorescent probes. *J. Agric. Food Chem.* **2000**, *48*, 328–334. [CrossRef]
28. Liu, S.F.; Sui, Y.; Guo, K.; Yin, Z.J.; Gao, X.B. Spectroscopic study on the interaction of pristine C_{60} and serum albumins in solution. *Nanoscale Res. Lett.* **2012**, *7*, 433. [CrossRef]